Hadrontherapy project ETOILE
Reconstruction of the slowly extracted beam

F. Méot
CEA, DSM/DAPNIA/SACM, 91191 Saclay
(fmeot@cea.fr)

August 22, 2002

Abstract

This report reviews the reconstruction of particle beams slowly extracted from the PIMMS synchrotron.

Report CEA DSM DAPNIA-02-176

Contents

Introduction

The Rhône-Alpes hadrontherapy project [1] is based on proton and Carbon beam delivery by slow extraction from a synchrotron, following the PIMMS design [2]. In this report we address the reconstruction of the slowly extracted beam at entrance to the extraction channel, in terms of horizontal and vertical phase spaces, momentum bite, extracted spill, losses, etc.

The goal is twofold : on the one hand review and understand PIMMS parameters and choices as to machine settings, within the frame of the Rhône-Alpes project "cahier des charges"and specificities [1], on the other hand produce realistic phase space distributions of the extracted beam, including in particular vertical motion, for assessment of initial conditions earlier high energy beam lines design is based on [3].

For the sake of precision tracking studies to follow are based on stepwise ray-tracing, which has the advantage of taking into account all sources of non linearities and coupling introduced by the dipole to sextupole magnets, particularly effective due to the large excursion of horizontal motion (separatrices) during extraction.

1 Extraction parameters, phase space geometry

The slow extraction process utilizes equipment displayed in Fig. 1 : a sextupole *XR* to excite the 1+2/3 resonance, a betatron core for pushing particles onto this resonance, so that these spiral out passed an electrostatic extraction septum *ES* into the extraction channel that eventually gets separated from the ring via a pair of magnetic septa *MS*.

Our working hypothesis are those of PIMMS extraction optics, that hold for both proton and Carbon beams. Strengths of the three PIMMS quadrupole families are, KF1 = 0.313571 m^{-2}, KF2 = 0.525158 m^{-2}, KD = -0.524811 m^{-2}. Fringe fields at dipole ends are included in the study however it can be shown that they are of little effect on extraction dynamics. Ensuing machine tunes are[1]

$$\nu_{x,0} = 1.666533, \quad \nu_{z,0} = 1.687982 \tag{1}$$

to be compared to regular matrix transport and derived data $\nu_{x,0} = 1.6666$, $\nu_{z,0} = 1.72$ as obtained with the same strengths [2, Part II],[5]. The difference (the most pronounced is in vertical tune) comes from the dipole fringe fields, however the vertical motion is of little effect on the extraction process and we choose to leave it as it is, keeping in mind that this mostly leads to (very) slightly different optical functions at the electrostatic extraction septum where further tracking data will be observed.

[1] As obtained from either multiturn Fourier analysis or from Twiss matrix calculation from one-turn paraxial ray transport.

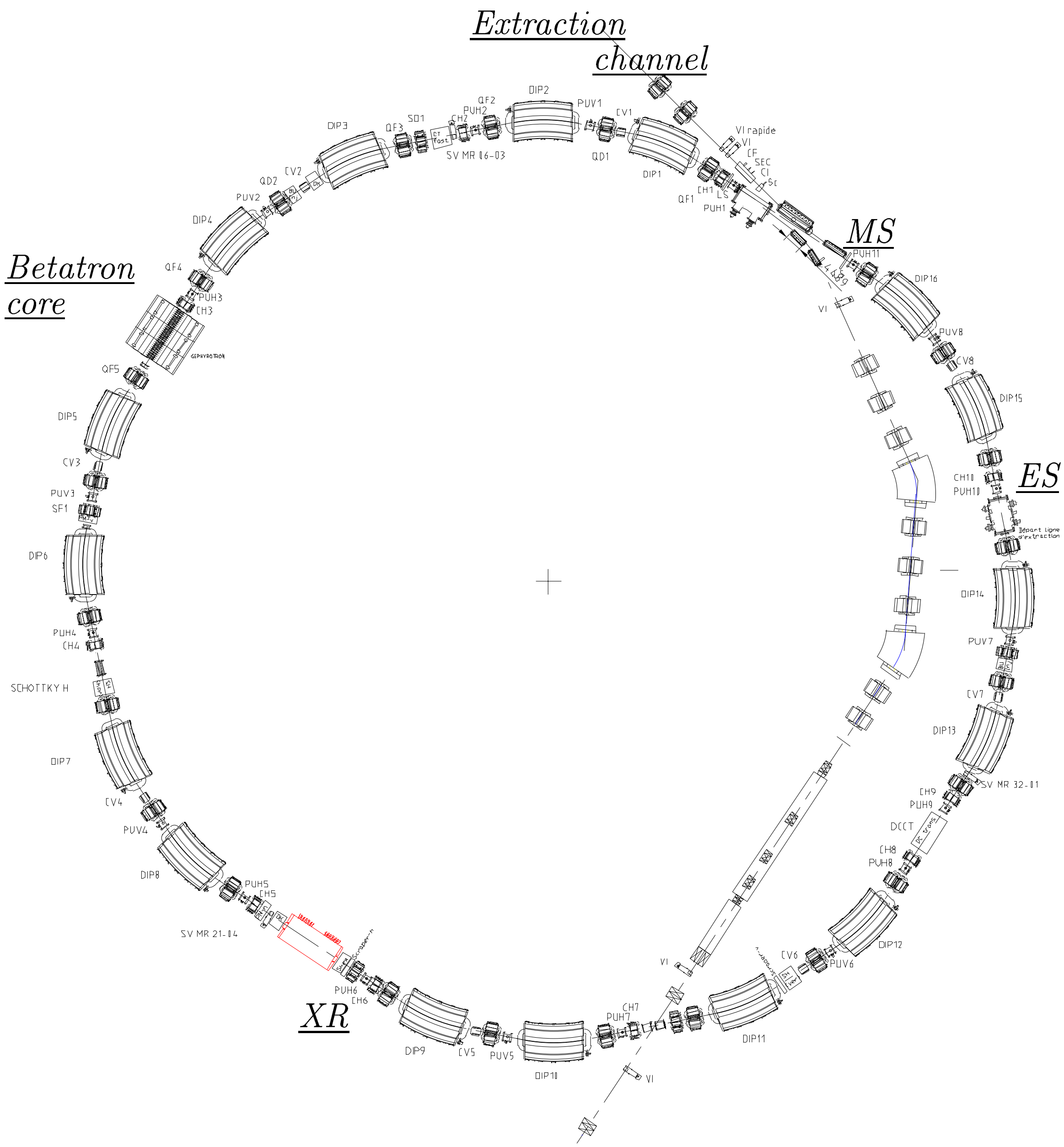

Figure 1: PIMMS ring [4], extraction equipment.

Optical functions are (ψ_x is the horizontal phase advance, origin taken at resonant sextupole *XR*) in particular D_x and D'_x at *ES* are tuned for overlapping of extraction separatrices (Eq. 5). All values are practically identical to PIMMS data [2, Part II,p.24,Fig.3.4] which allows further precise comparisons.

	β_x	α_x	D_x	D'_x	ψ_x	β_z	α_z
Middle of *XR*	8.49	-0.172	0	0	0	3.73	-0.497
Entrance of *ES*	16.37	0.398	3.87	-0.62	3.974	6.38	-0.13
Entrance of *MS*	8.50	0.198	0	0	4.869	3.79	0.507

Chromaticity sextupole strengths are[2], S_F = 0.240618 m^{-3}, S_D = -0.89269 m^{-3} (length = 0.2m) yielding

$$\xi_x = d\nu_x/dp/p = -3.696, \quad \xi_z = d\nu_z/dp/p = -1.113 \tag{2}$$

which compares well enough with Ref. [2, Part II,Sec.3.11,p.69] values $\xi_x = -3.655$ and $\xi_z = -1.158$. The resonant sextupole strength upon extraction is $S_{XR} = -5.35$ m^{-3}, length = 0.2 m.

Largest stable emittance

Prior to multiparticle simulations we check the basic parameters of slow extraction dynamics. At the resonant sextupole the largest stable triangle height H and base B (upright in Fig. 2) are

$$H = 12\pi\frac{\nu_x - \nu_{x,R}}{S}\sqrt{\beta_{x,XR}}\ , \quad B = 8\pi\sqrt{3}\frac{\nu_x - \nu_{x,R}}{S}/\sqrt{\beta_{x,XR}} \tag{3}$$

wherein ν_x = particle tune, $\nu_{x,R}$ = resonant tune, $S = \beta_{x,XR}^{3/2} S_{XR} L$ with L = magnetic length (from previous data, $S = 27.95$ m$^{-1/2}$). The emittance $A/\pi = H \times B/2/\pi$ of the triangle ensues, namely

$$A/\pi = 48\pi\sqrt{3}\left(\frac{\nu_x - \nu_{x,R}}{S}\right)^2 \tag{4}$$

Eq. 4 shows that the surface A shrinks under the effect of the betatron core acceleration that pushes particles onto the resonance by causing $\nu_x \to \nu_{x,R}$ (whereas the sextupole strength S is kept unchanged). Theoretical values ensuing from Eqs. 3, 4 are gathered in Tab. 1 where they can be compared with those obtained from numerical simulations shown in Fig. 2.

Phase advances as drawn from the numerical simulations, i.e. as well separatrix rotation as observed in Fig. 2, amount to

228 deg at electrostatic septum (*ES*)

279 deg at magnetic septum (*MS*)

with respect to the extraction sextupole (*XR*), hence a 51 deg phase advance from *ES* to *MS*, all values in excellent agreement with [2, Part II,p.24,Fig.3.4].

[2] $S = B_{pole-tip}/(B\rho\ radius^2_{pole-tip})$

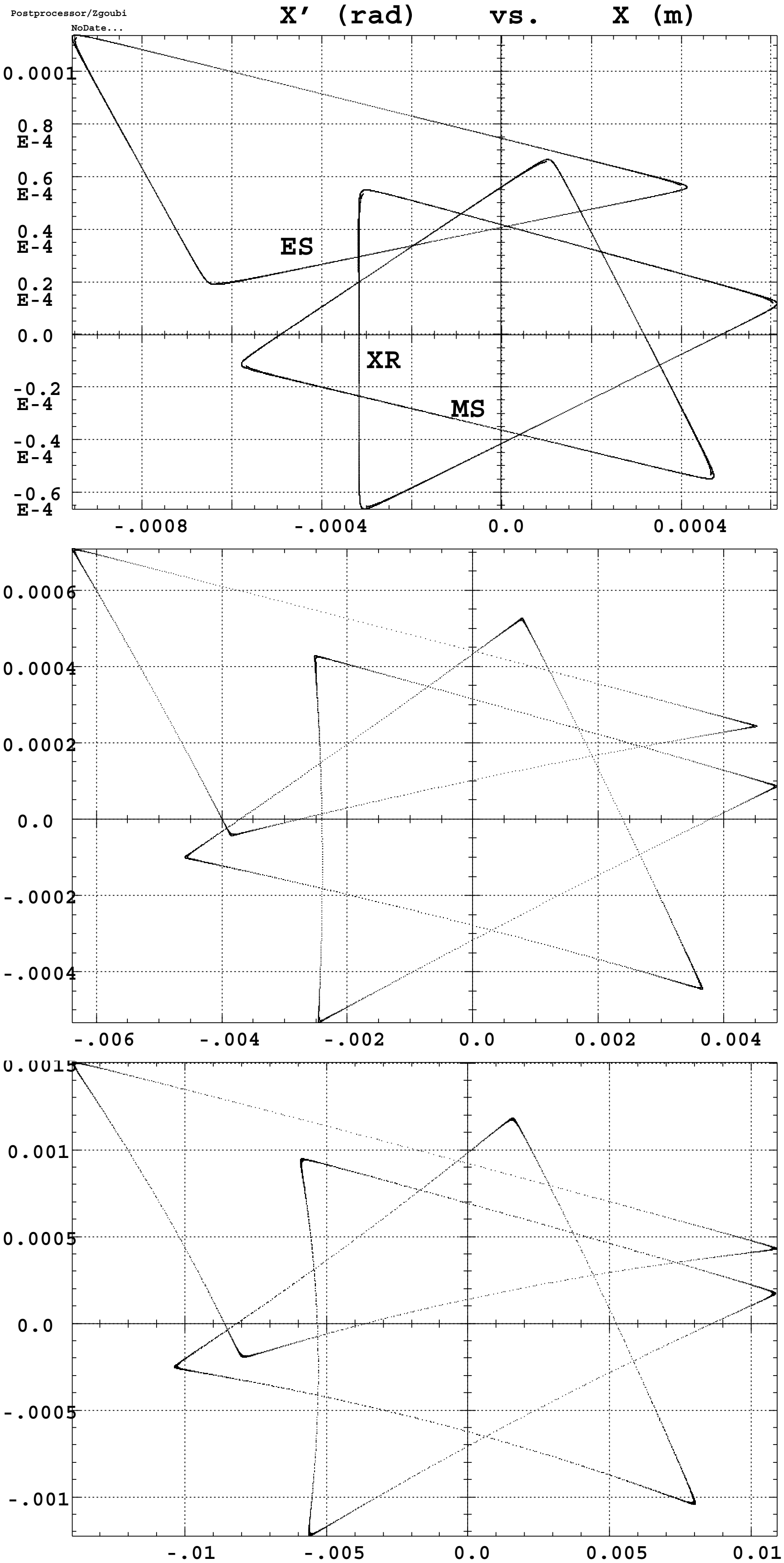

Figure 2: Observation at resonant sextupole (*XR*), electrostatic extraction septum (*ES*) and magnetic extraction septum (*MS*). Top plot : $p/p_0 = 0.9999$; middle : $p/p_0 = 0.9995$; bottom : $p/p_0 = 0.999$.

Table 1: Emittance A/π (cols. 3,4) of the largest stable triangle as a function of momentum deviation dp/p (col. 1).

dp/p	$\nu_x^{(a)}$	A/π ($\times 10^{-6}$) tracking$^{(b)}$	A/π ($\times 10^{-6}$) Eq. 4	H ($\times 10^{-3}$) tracking	H ($\times 10^{-3}$) Eq. 3	B ($\times 10^{-4}$) tracking	B ($\times 10^{-4}$) Eq. 3
0.9999	0.66692	0.017/0.0174	0.018	0.93	0.95	1.21	1.24
0.9995	0.66841	1.11/1.10	1.06	7.27	7.12	9.60	9.34
0.999	0.67035	5.66/5.48	5.16	16.4	15.7	21.7	20.6

$^{(a)}$ From Fourier analysis of the unperturbed phase space motion, or with better than 10^{-4} agreement from $\nu_x = \nu_{x,0} + \xi_x \frac{dp}{p}$

$^{(b)}$ Left hand value, approximate, after geometry : $H * B/2/\pi$; right hand value more precise, from ellipse fit, XR off (see App. B).

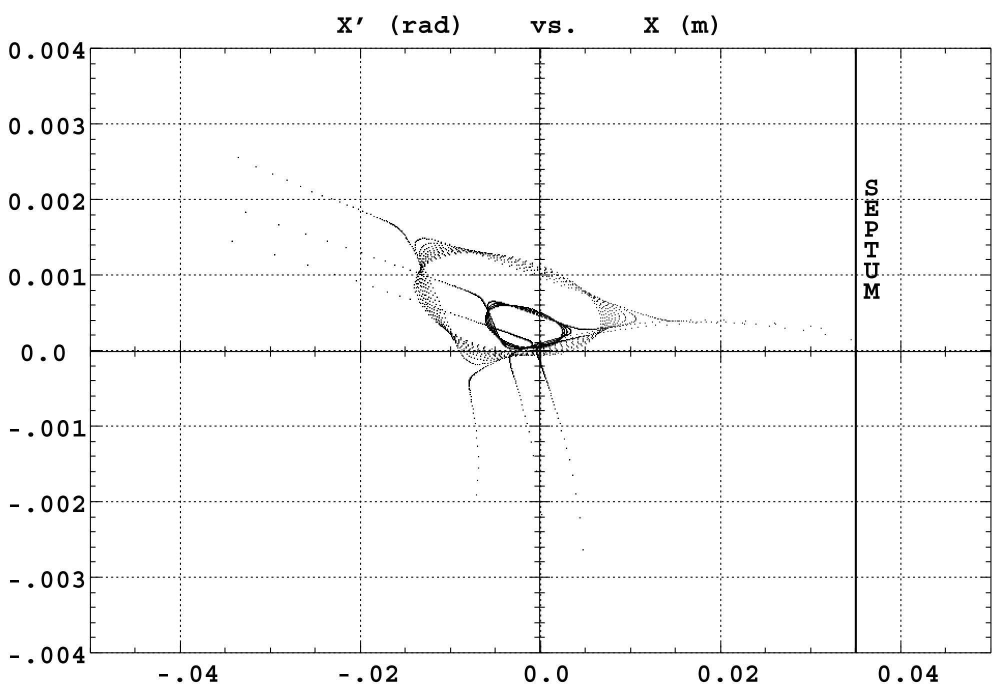

Figure 3: Alignment of extraction separatrices (starting from linear motion) for $p/p_0 = 0.9999, 0.9995$, and 0.999.

Alignment of separatrices

Alignment of the extraction separatrices for all momenta as schemed in Fig. 3 (obtained with the present settings, page 3, consistent with [2, Part II,p.25,Fig.3.5]) is realized through the condition

$$\frac{\alpha_x D_x + \beta_x D'_x}{\sqrt{\beta}} \sin(\phi + \frac{\pi}{3}) + \frac{D_x}{\sqrt{\beta}} \cos(\phi + \frac{\pi}{3})\bigg|_{ES} = -\frac{4\pi}{S}\xi_x. \tag{5}$$

that is fairly satisfied given $\beta_x =$, $\alpha_x =$, $D_x =$, $D'_x =$. Amongst others, one effect of that alignment relevant to the extracted beam is to reduce the angle spread $\Delta x'$ on the external side of the septum and therefore the overall extracted horizontal emittance. A consequence of reduced $\Delta x'$ is to minimize particle losses on the septum.

The chromaticity ξ_x is used for controlling the alignment.

Spiral step

The maximum spiral step remains unchanged all along the extraction process since the sextupole strength is maintained constant - this is one interest of the tune distance shrinking via betatron core acceleration (Eq. 4).

2 Extraction trials

2.1 2D+dp/p

A 2000 particle beam is launched for extraction over about 10^4 turns. Fig. 4 shows the initial horizontal conditions as observed at the electrostatic extraction septum, the vertical motion is null. Fig. 5 shows the momentum distribution over $dp/p = (-3 \pm 2)\ 10^{-3}$ total ; the $< dp/p >= -3\ 10^{-3}$ average off-centering causes local shift of the beam centroid that amounts to $(D_x\ dp/p, D'_x\ dp/p) =$ (-0.0116 m,0.0018 rad) ; the corresponding horizontal tune is $\nu_x = \nu_{x,0} + \xi_x dp/p = 1.677762$ (Eqs. 1, 2) whereas particles closest to $\nu_{x,R} = 1 + 2/3$ have $dp/p = (-3+2)\ 10^{-3} = -10^{-3}$ and $\nu_x = \nu_{x,0} + \xi_x dp/p = 1.67023$. Note that, given that the amplitude detuning is positive particles with non-zero betatron amplitude are shifted away from $\nu_x = 1.67023$ and hence from $\nu_{x,R}$.

Tracking starts with adiabatic switch of the extraction sextupole within a few hundred turns up to its nominal strength. The betatron yoke is then fired, it is simulated here with a dp/p=0.6 10^{-6} kick per turn, extraction proceeds until the beam is fully peeled off. Typical tracking data used for these simulations can be found in App. A. A few tracking results are summarized in Fig. 6 that shows the survival rate in the ring, together with the extracted spill and in Fig. 7 that schemes the particle dynamics in the horizontal phase space.

The resulting horizontal phase space of the extracted beam is shown in Fig. 8 ; the transverse horizontal extent (maximum spiral step) comes out to be 9.50 10^{-3} m fairly close to the 10 mm expected value. an elliptical border with $0.2\pi\ 10^{-6}$ m.rad emittance, $\beta_x = 125$ m/rad, $\alpha_x = -1.4$ is superimposed ; this is for comparison with Ref. [3] where the design of the high energy beam lines that take the beam to

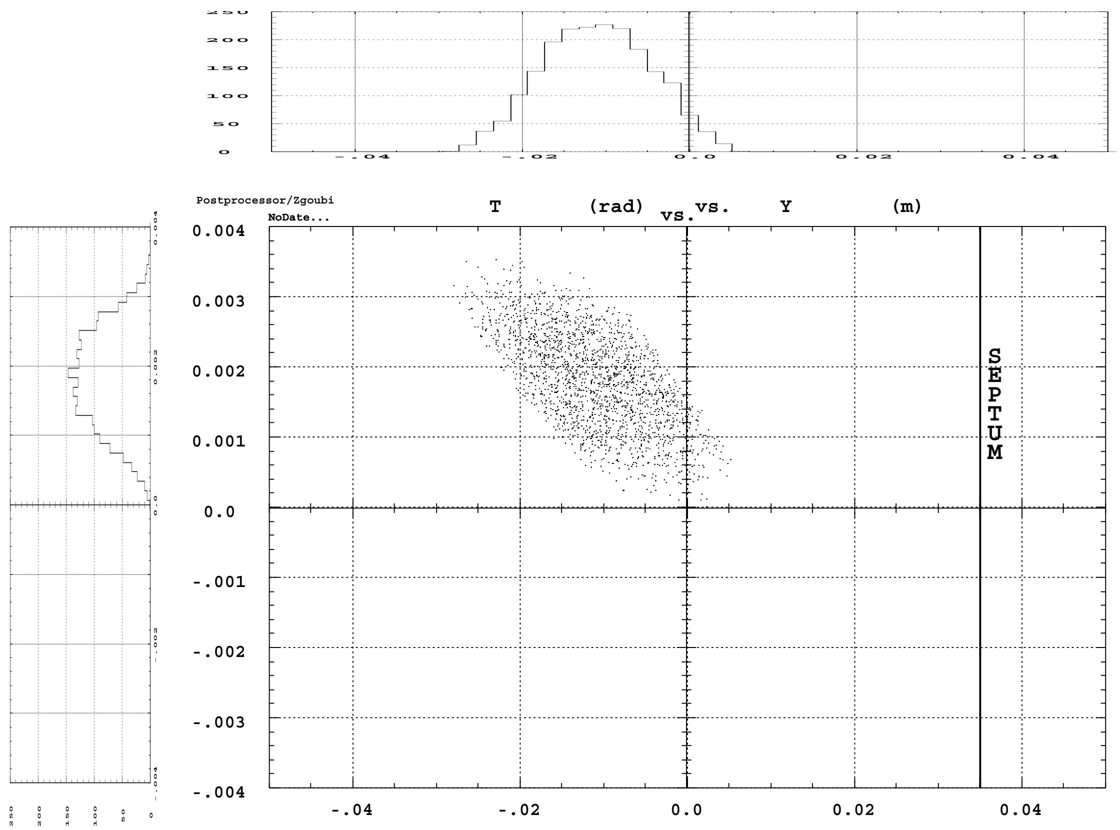

Figure 4: Launch conditions prior to extraction process : horizontal phase space at electrostatic extraction septum, sextupole off.

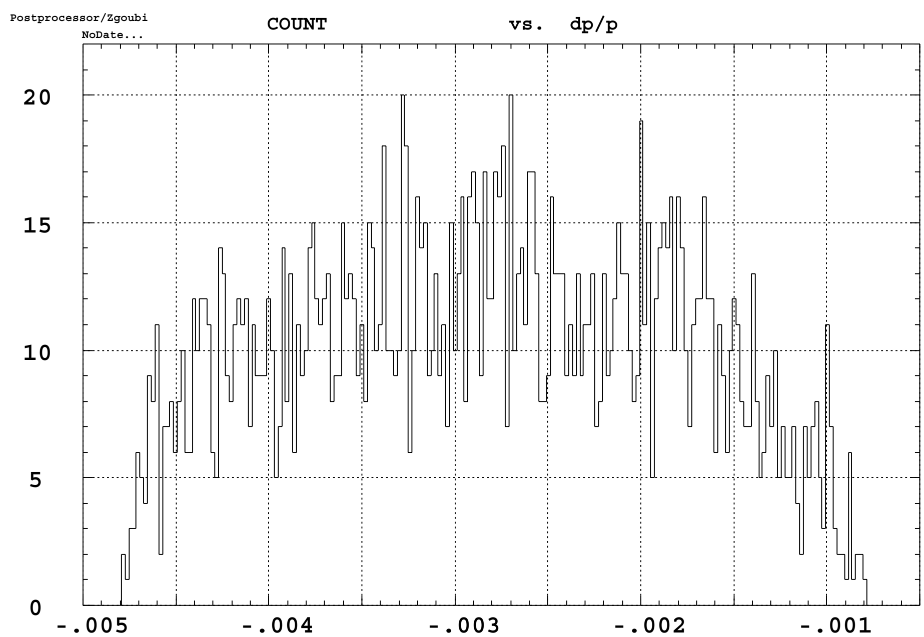

Figure 5: Launch conditions prior to extraction process : initial momentum distribution, with $dp/p = (-3 \pm 2)\ 10^{-3}$ total.

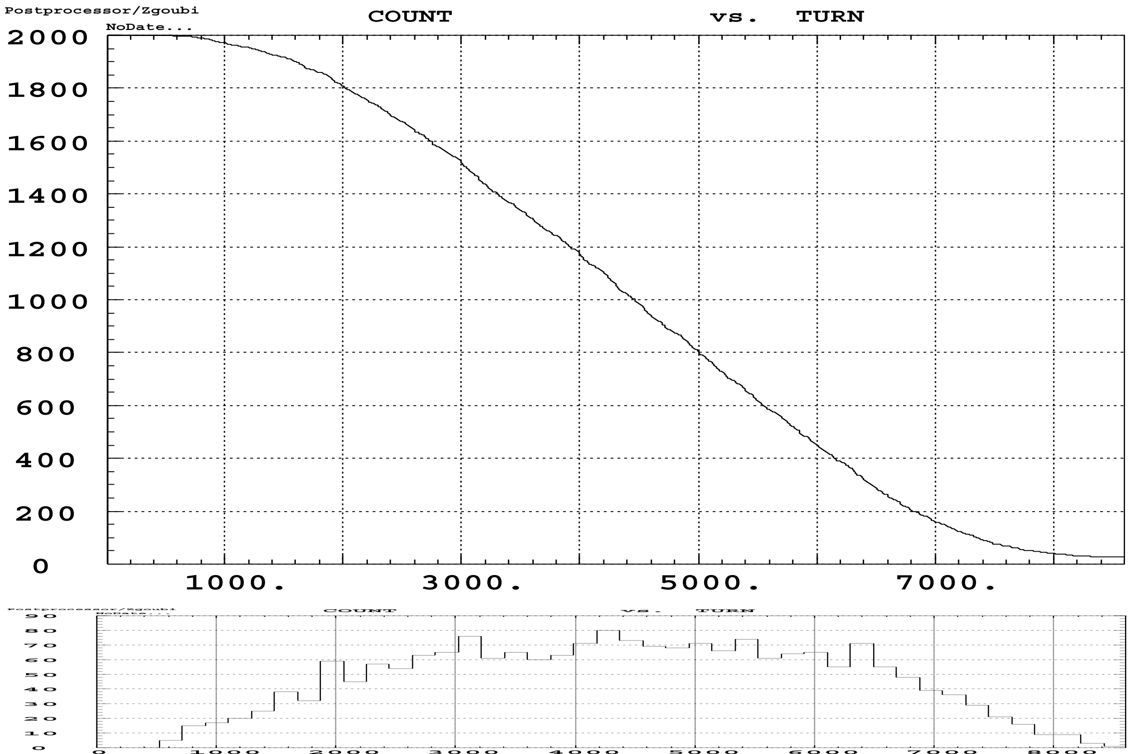

Figure 6: Top : particles remaining in the ring vs. turn number. Bottom : extracted spill (number of extracted particles vs. turn number).

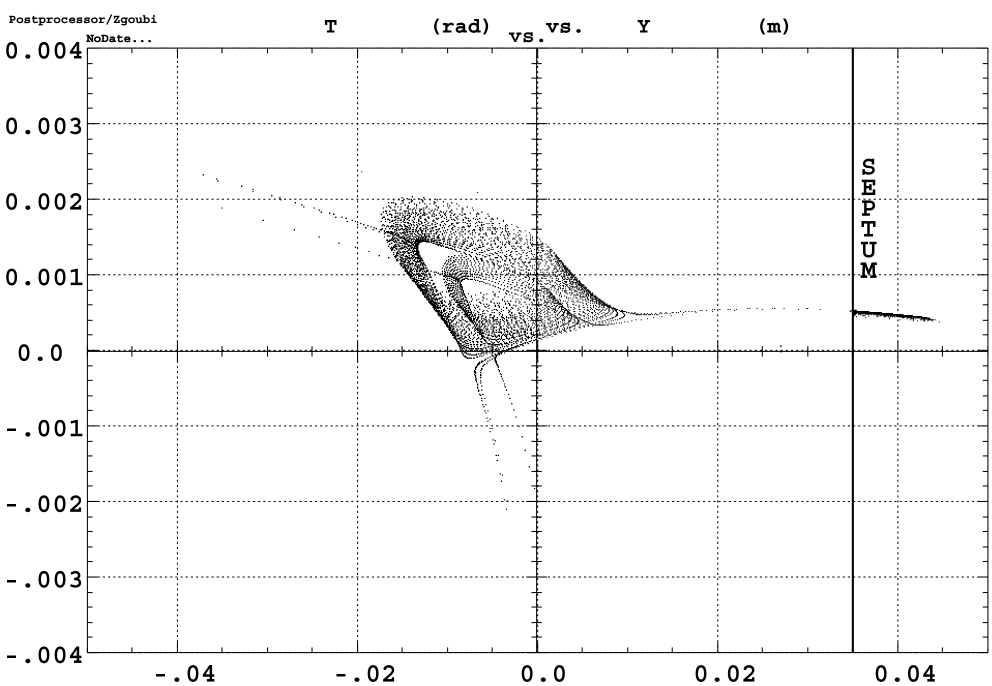

Figure 7: Horizontal phase space motion of a few particles up to the extraction septum (vertical solid line at x = 0.035 m) ; the full extracted beam is also shown on the right side of the extraction septum.

the treatment rooms (HEBT) is performed on $\epsilon_x/\pi = 0.2\ 10^{-6}$ m.rad and on beam conditions at start of the extraction channel $\beta_x = 125$ m/rad and $\alpha_x = 0$. That question is addressed in more details in Section 2.2, the main remark for the moment is that the matching in the absence of vertical motion is good.

The extracted and stored emittances and momentum spread are related by[3] [2, PartII]

$$\epsilon_x \times dp/p|_{extracted} \times T_{spill} = \epsilon_x \times dp/p|_{stored} \times T_{rev}$$

from what the theoretical value of the extracted emittance ensues, $\epsilon_x/\pi|_{extracted} \approx 4\ 10^{-9}$ m.rad (given $\epsilon_x/\pi_{stored} = 7.14\ 10^{-6}$, $dp/p|_{stored} = 4\ 10^{-3}$ total, $T_{spill} = 6\ 10^3\ T_{rev}$ (Fig. 6)) more 50 times smaller than simulation result $\approx 2\ 10^{-7}$ m.rad. Amongst others one reason for that discrepancy is in the loose overlapping of extraction separatrices, as clearly appears in Fig. 3.

2.2 4D+dp/p

Horizontal conditions at extraction septum at launch are identical to the previous ones (Fig.4), initial vertical conditions are shown in the Figure aside ($\epsilon_z/\pi = 7.15\ 10^{-6}$ m.rad, $\beta_z = 6.35$ m/rad, $\alpha_z = 0.19$, see p. 5). The resulting phase spaces of the extracted beam are shown in Fig. 11 ; the transverse horizontal extent (maximum spiral step) comes out to be 9.50 10^{-3} m fairly close to the 10 mm expected value. The design of the high energy beam lines reported in Ref. [3] is performed with slightly different beam values : such slight discrepancies in β, α values

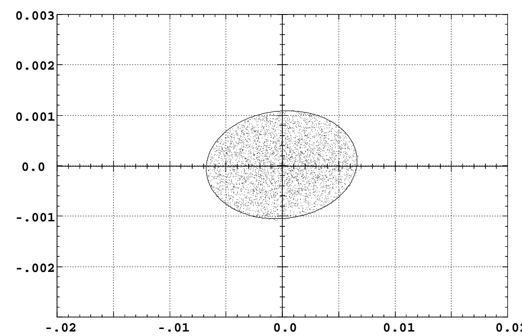

Figure 10: Initial vertical conditions of a 2000-particle beam.

	ϵ_x/π	β_x	α_x	ϵ_z/π	β_z	α_z
Reconstructed (Fig. 11)	0.2 10^{-6}	125	-1.4	7.15 10^{-6}	10.4	-0.351
Ref. [3]	0.2 10^{-6}	125	0	7.15 10^{-6}	6.52	-0.17

can easily be handled by the adaptation optics of the upstream section of the HEBT (so-called "extraction section"), on the other hand as concerns the horizontal emittance it can be figured out from Fig. 8 that slightly larger should be considered which however does not affect the design in Ref. [3] considering the comfortable safety margins taken for establishing optical aperture along the lines from envelope calculations.

[3]Another estimate can be drawn from [7] $\epsilon_x/\pi|_{extracted} \approx \Delta X' \times$ max. spiral step

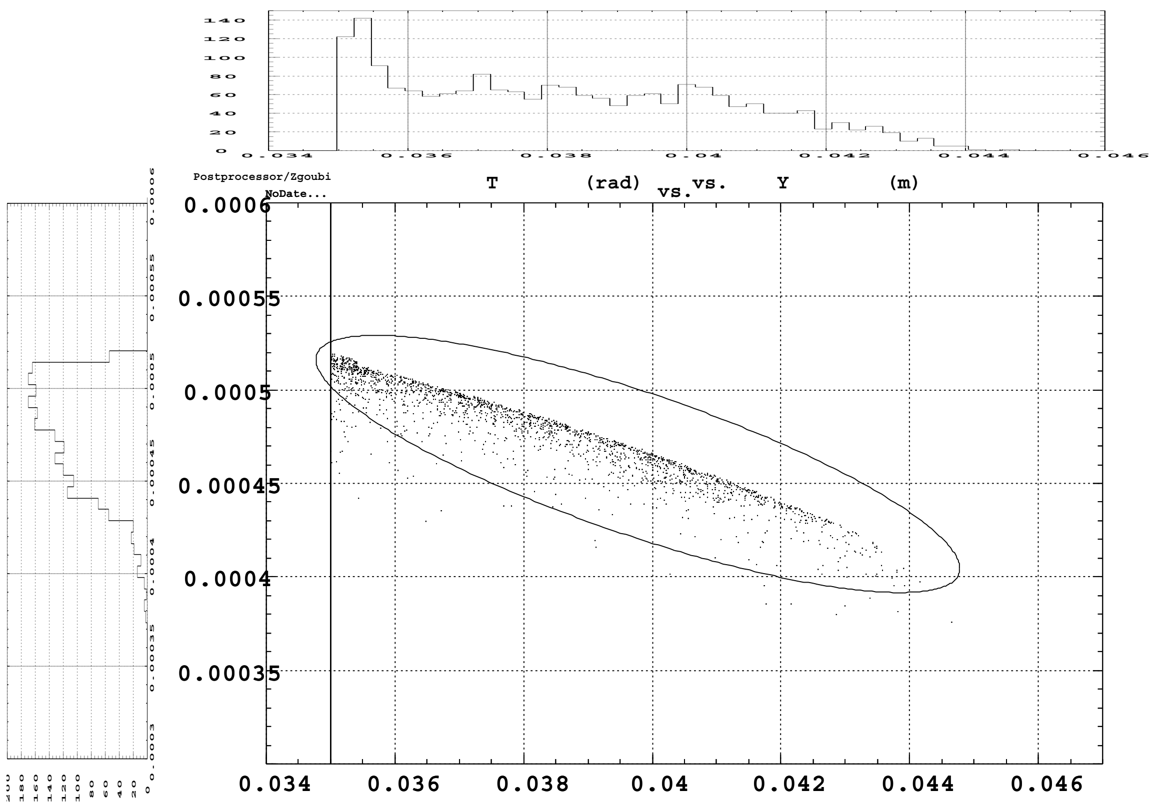

Figure 8: Horizontal phase space of the extracted beam at entrance to the extraction electrostatic septum and $0.2\pi\ 10^{-6}$ m.rad elliptical border.

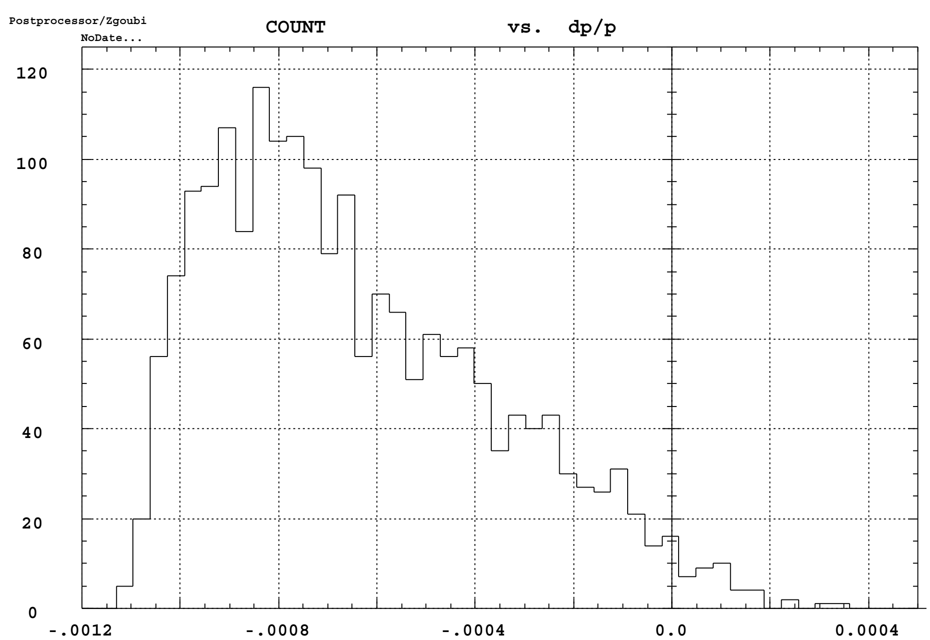

Figure 9: Momentum histogram of extracted beam. min -0.00111020994 , max 3.4687693244E-04. Mean:-6.41183E-04; Sigma: 2.99741E-04; X(max):-7.30330E-04 dp/p=0 refers to on-momentum particle in the ring.

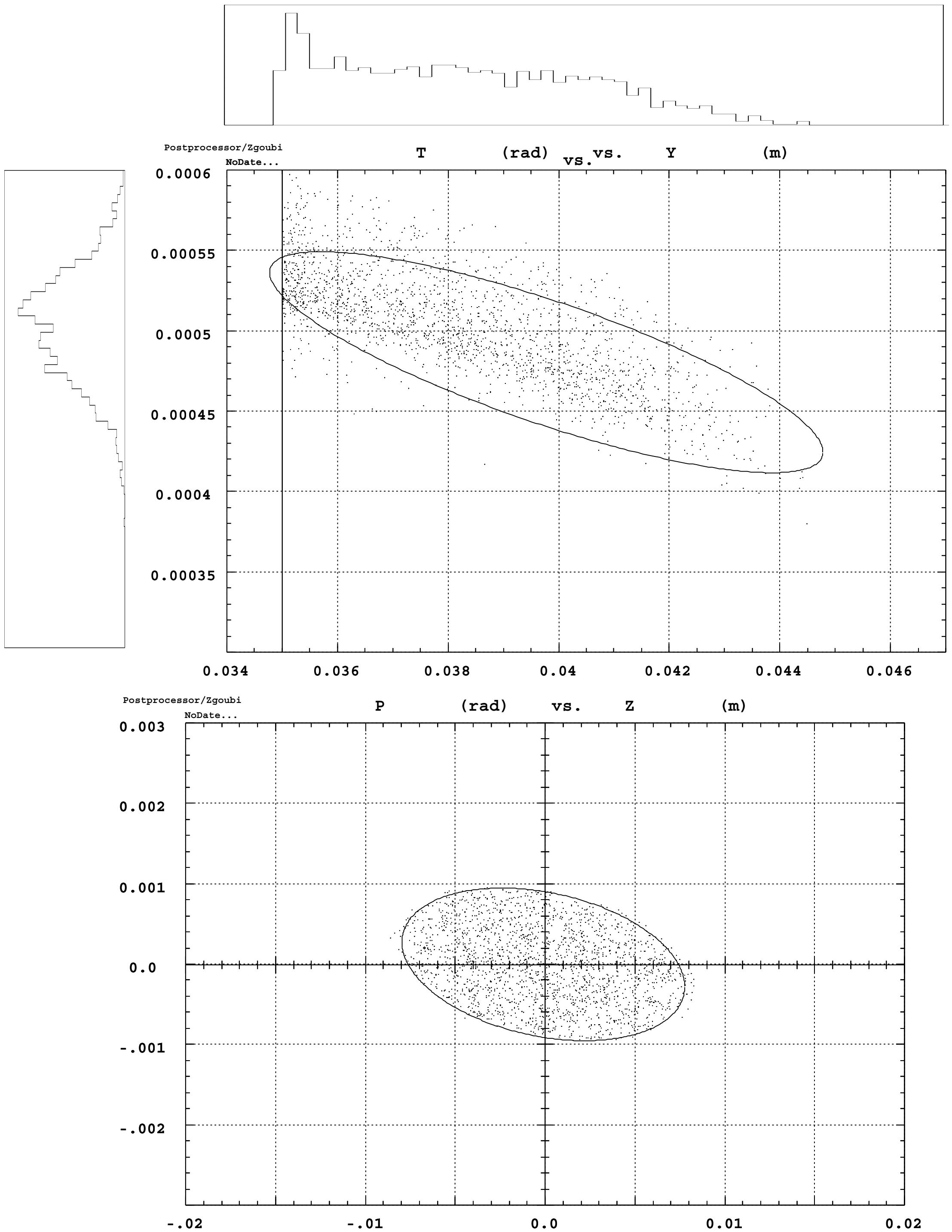

Figure 11: Details on the extracted beam at entrance to the extraction channel (electrostatic septum). Top : horizontal phase space, $\epsilon_x/\pi = 0.2\ 10^{-6}$ m.rad border with $\beta_x = 125$ m/rad, $\alpha_x = -1.4$. Bottom : matching ellipse with $\epsilon_z/\pi = 7\ 10^{-6}$ m.rad, $\beta_z = 10.4$ m/rad, $\alpha_z = -0.351$.

10^5 turns extraction

Too large number of turns, motion including vertical component is not symplectic, see Fig. 18 in App. C.

Horizontal and vertical conditions at extraction septum at launch are identical to the previous ones (Figs.4, 10).

The resulting phase spaces of the extracted beam are shown in Fig. 14 ; the transverse horizontal extent (maximum spiral step) comes out to be 9.50 10^{-3} m. Fig. 15 shows the momentum spread of the extracted beam.

3 Comments

The following remarks come out.

It is observed that less than 40/1000 losses occur along the machine during extraction cycle, all other particles leave the ring chamber through the extraction channel, which confirms that separatrices are within transverse acceptance up to the electrostatic septum.

A zero thickness septum has been considered, simulation of extraction efficiency would require allowing for true value.

Beam envelopes in the HEBT can be generated from realistic extracted phasesspaces such as derived here.

Results with non-zero ϵ_z have been compared with Cern report 2000-006 [7]. Agreement in the x' displacement of the separatrix when introducing z motion is found ; also unchanged maximum spiral step is observed here whatever ϵ_z, as expected.

Note a change in the optical functions of the extracted z-ellipse (Fig. 11) whereas emittance is preserved, i.e. the ellipse is titled wrt. the periodic ellipse at ES(Fig. 10), due momentum detuning.

Acknowledgements

Thanks to A. Tkatchenko (IPN-Orsay) for help and advices.

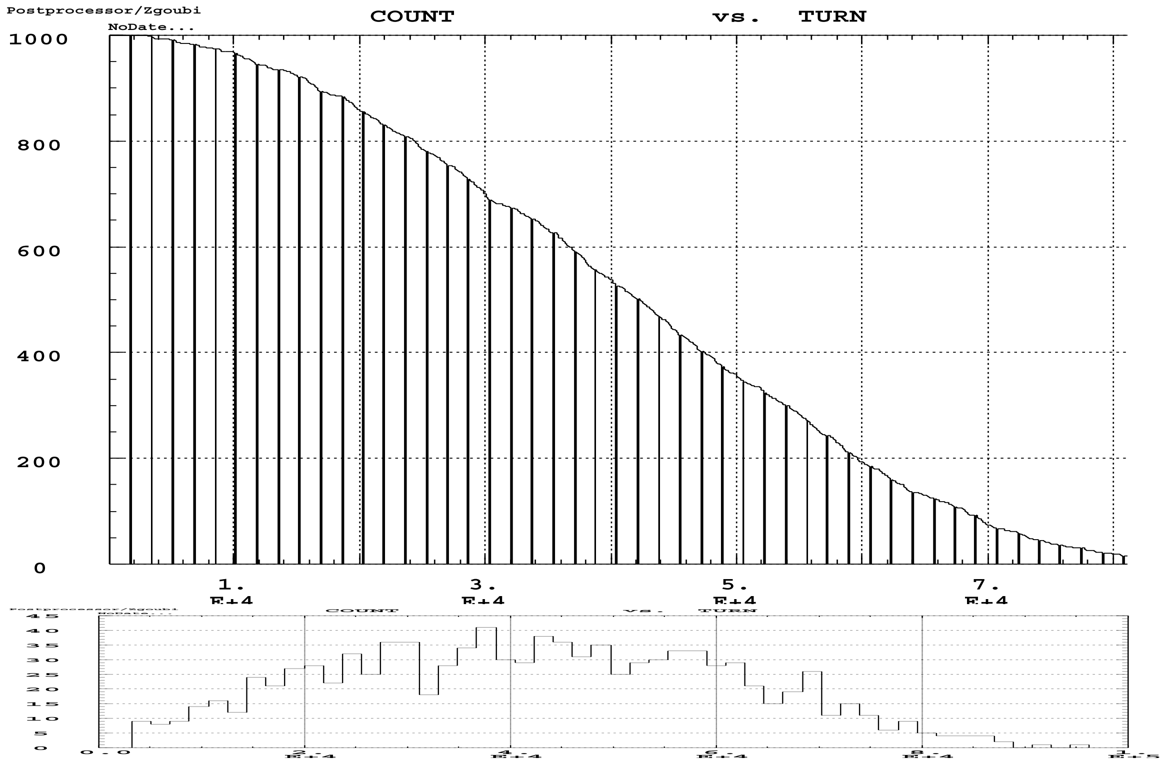

Figure 12: Top : particles remaining in the ring vs. turn number. Bottom : extracted spill (number of extracted particles vs. turn number).

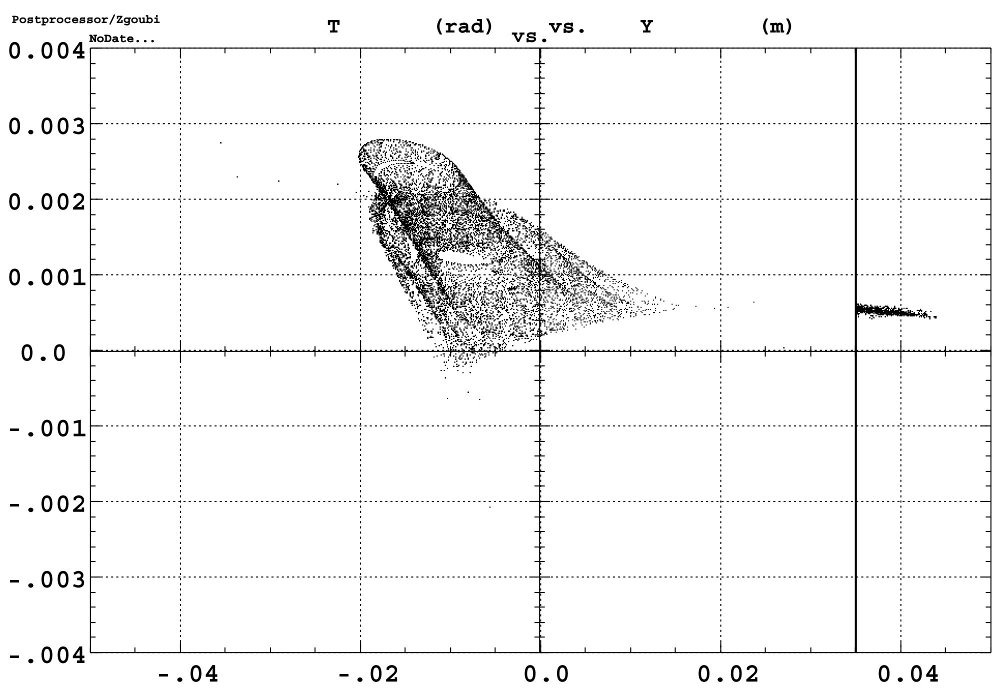

Figure 13: Horizontal phase space motion of a few particles up to the extraction septum ; the full extracted beam is also shown on the right side of the extraction septum, maximum x-extent is .035→.0439 m.

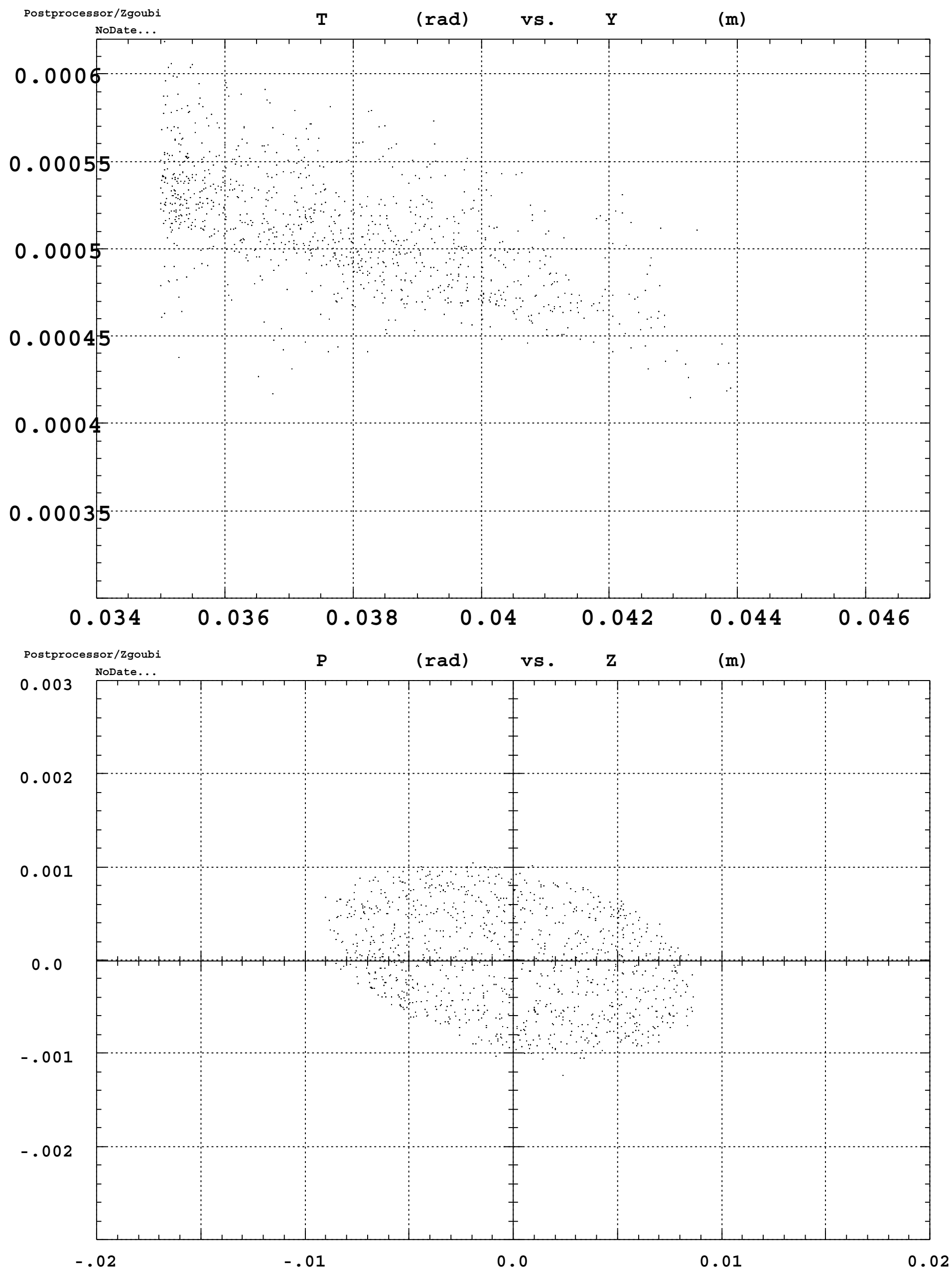

Figure 14: Details on the extracted beam at entrance to the extraction channel (electrostatic septum). Top : horizontal phase space ; bottom : vertical.

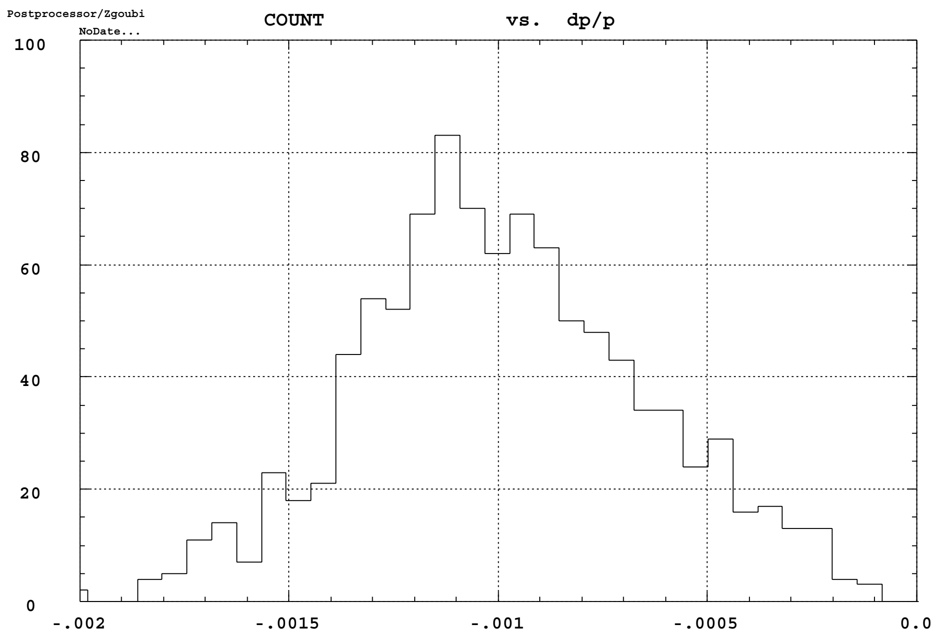

Figure 15: Momentum histogram of extracted beam. dp/p=0 refers to on-momentum particle in the ring.

A Typical tracking data

```
 'MCOBJET'  objet pour extraction C6+ 120MeV/u
 1000.
  3
 2000
 2 2  1 1 1 1
  0. 0. 0. 0. 0.  0.997
 0. 8.562  7.143E-6  1
 0. 2.848  7.143E-6  1
 0. 1.     4.E-6     1
 123456 234567 345678
   'SCALING'
  1  2
   MULTIPOL   XR_
 3
 0  1    1
 1  400  99999
 BETATRON
   4
 0. 0.   1    1
 1  400  401  999999
'FAISTORE'  lmnt#
b_xtract.fai   ESE_ICOL
 10
'BETATRON'
 0.6e-6
'DRIFT'  SS_MR_01_03 Here, betx=8.562,betz=2.848
     75.0000
'COLLIMA'  ESi_COL
1
 1 5.8   3.7   1.7 0.        1.7-5.8=-4.1, 1.7+5.8=7.5
'DRIFT'    DRIF      ES_INJECTION
     15.0000
'DRIFT'    DRIF      ES_INJECTION
     15.0000
'DRIFT'    DRIF      ES_INJECTION
     15.0000
'DRIFT'    DRIF      ES_INJECTION
     15.0000
'COLLIMA'  ESi_COL
1
 1 5.8   3.7   1.7 0.        1.7-5.8=-4.1, 1.7+5.8=7.5
'DRIFT'    ESinj DRIF      SS_MR_01_04
     95.0000
'MULTIPOL' QUAD      QF_1
0  .Quad
   17.5000 10.00 .0000000000 .313571  .0  .0  .0  .0  .0  .0  .0  .0
0. 0. 6.0 5.60  1.00 0.00 0.00 0.00 0.00 0. 0. 0. 0.
6 -.010967  5.464823  .996848 1.568787 -5.671630 18.505734
0. 0. 6.0 5.60  1.00 0.00 0.00 0.00 0.00 0. 0. 0. 0.
6 -.010967  5.464823  .996848 1.568787 -5.671630 18.505734
 0. 0. 0. 0. 0. 0. 0. 0. 0. 0.
4.010E10  3.600 cm   Quad   QF_1
1 0. 0. 0.
'COLLIMA'   Q_COL
1
1 7. 3.7  0.  0.
'MULTIPOL' QUAD      QF_1
0  .Quad
   17.5000 10.00 .0000000000 .313571  .0  .0  .0  .0  .0  .0  .0  .0
0. 0. 6.0 5.60  1.00 0.00 0.00 0.00 0.00 0. 0. 0. 0.
6 -.010967  5.464823  .996848 1.568787 -5.671630 18.505734
0. 0. 6.0 5.60  1.00 0.00 0.00 0.00 0.00 0. 0. 0. 0.
6 -.010967  5.464823  .996848 1.568787 -5.671630 18.505734
 0. 0. 0. 0. 0. 0. 0. 0. 0. 0.
4.010E10  3.600 cm   Quad   QF_1
1 0. 0. 0.
'DRIFT'    DRIF      SS_MR_02
     33.2000
'COLLIMA'   B_COL
1
1 7. 3.2  0.  0.
'MULTIPOL' SBEN      MB
0  .Dip
 165.0348  10.00 2.36423288 .00000000 .00000000  .0  .0  .0  .0  .0  .0
14.00 11.  0.00 0.00 0.00 0.00 0.00 0. 0. 0. 0.
6 .015527 3.874961 -2.362230 2.978209 12.604429 15.025689
14.00 11.  0.00 0.00 0.00 0.00 0.00 0. 0. 0. 0.
6 .015527 3.874961 -2.362230 2.978209 12.604429 15.025689
 0. 0. 0. 0. 0. 0. 0. 0. 0. 0.
6.020E10  FFDip   12.020E10  Dip     5.015E10    Dip   MB
             3 0.    .0000000000E+00    .0000000000E+00
'COLLIMA'   B_COL
1
1 7. 3.2  0.  0.
'DRIFT'    DRIF      SS_MR_03
     56.2000
'MULTIPOL' QUAD      QD
0  .Quad
   17.5000 10.00 .0000000000 -.524811 .0  .0  .0  .0  .0  .0  .0  .0
0. 0. 6.0 5.60  1.00 0.00 0.00 0.00 0.00 0. 0. 0. 0.
6 -.010967  5.464823  .996848 1.568787 -5.671630 18.505734
0. 0. 6.0 5.60  1.00 0.00 0.00 0.00 0.00 0. 0. 0. 0.
6 -.010967  5.464823  .996848 1.568787 -5.671630 18.505734
 0. 0. 0. 0. 0. 0. 0. 0. 0. 0.
4.010E10  3.600 cm   Quad   QD
1 0. 0. 0.
'COLLIMA'   Q_COL
 1
1 7. 3.7  0.  0.
-----------------------------------------------------------
'MULTIPOL' SEXT      XC_F
0  .Sext
   20.0000 10.00 .0000 .0000     .0240618  .0  .0  .0  .0  .0  .0  .0
0.00 0.00  1.00 0.0 .0 0.0 .0 0.0 .0 0.0 .0
6 -.010967  5.464823  .996848 1.568787 -5.671630 18.505734
0.00 0.00  1.00 0.0 .0 0.0 .0 0.0 .0 0.0 .0
6 -.010967  5.464823  .996848 1.568787 -5.671630 18.505734
 0. 0. 0. 0. 0. 0. 0. 0. 0. 0.
5.010E10  Sext
1 0. 0. 0.
'COLLIMA'   H_COL
1
1 7. 3.7  0.  0.
-----------------------------------------------------------
'MULTIPOL'   XR_
0  .Sext
   10.0000 10.00   .0000 .0000 -.535  .0  .0  .0  .0  .0  .0  .0
0.00 0.00  1.00 0.0 .0 0.0 .0 0.0 .0 0.0 .0
6 -.010967  5.464823  .996848 1.568787 -5.671630 18.505734
0.00 0.00  1.00 0.0 .0 0.0 .0 0.0 .0 0.0 .0
6 -.010967  5.464823  .996848 1.568787 -5.671630 18.505734
 0. 0. 0. 0. 0. 0. 0. 0. 0. 0.
5.010E10  Sext
1 0. 0. 0.
'DRIFT'   XR_Med
0.
'MULTIPOL'   XR_
0  .Sext
   10.0000 10.00   .0000  .0000 -.535  .0  .0  .0  .0  .0  .0  .0
0.00 0.00  1.00 0.0 .0 0.0 .0 0.0 .0 0.0 .0
6 -.010967  5.464823  .996848 1.568787 -5.671630 18.505734
0.00 0.00  1.00 0.0 .0 0.0 .0 0.0 .0 0.0 .0
6 -.010967  5.464823  .996848 1.568787 -5.671630 18.505734
 0. 0. 0. 0. 0. 0. 0. 0. 0. 0.
5.010E10  Sext
1 0. 0. 0.
'COLLIMA'   H_COL
 1
1 7. 3.7  0.  0.
-----------------------------------------------------------
'MULTIPOL' SEXT      XC_D
0  .Sext
   20.0000 10.00  .0000  .0000  -.089269  .0  .0  .0  .0  .0  .0  .0
0.00 0.00  1.00 0.0 .0 0.0 .0 0.0 .0 0.0 .0
6 -.010967  5.464823  .996848 1.568787 -5.671630 18.505734
0.00 0.00  1.00 0.0 .0 0.0 .0 0.0 .0 0.0 .0
6 -.010967  5.464823  .996848 1.568787 -5.671630 18.505734
 0. 0. 0. 0. 0. 0. 0. 0. 0. 0.
5.010E10  Sext
1 0. 0. 0.
'COLLIMA'   H_COL
 1
1 7. 3.7  0.  0.
'DRIFT'    DRIF      SS_MR_26_02
     20.0000
'MULTIPOL' QUAD      QF_2
0  .Quad
   17.5000 10.00  .0000000000 .525158  .0  .0  .0  .0  .0  .0  .0  .0
0. 0. 6.0 5.60  1.00 0.00 0.00 0.00 0.00 0. 0. 0. 0.
6 -.010967  5.464823  .996848 1.568787 -5.671630 18.505734
0. 0. 6.0 5.60  1.00 0.00 0.00 0.00 0.00 0. 0. 0. 0.
6 -.010967  5.464823  .996848 1.568787 -5.671630 18.505734
 0. 0. 0. 0. 0. 0. 0. 0. 0. 0.
4.010E10  3.600 cm   Quad   QF_2
1 0. 0. 0.
-----------------------------------------------------------
'DRIFT'    DRIF      SS_MR_01_02
   109.4000
'FAISCEAU'  #END
'REBELOTE'
  9999 0.1  99
'END'
```

B Tracking accuracy

A question of strong concern in such highly non-linear tracking is that of accuracy. Various types of tests can be performed, two examples are given here after.

Fig. 16 shows the fair behaviour of 5000-turn tracking of a few particles $dp/p = -10^{-3}$ off-momentum in the vicinity of their limit stable triangle, as observed at the extraction septum[4].

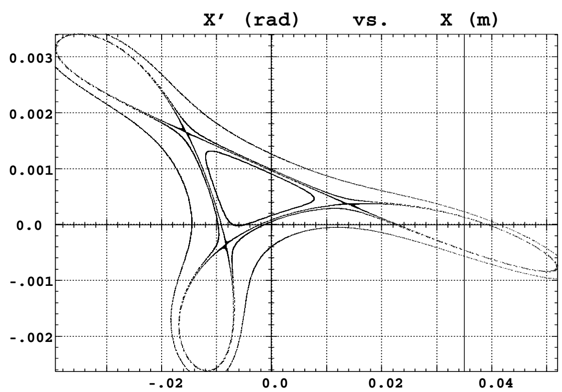

Figure 16: Motion in the vicinity of the separatrix for $p/p_0 = 0.999$ (hence $\nu_x - \nu_{x,R} > 0$), observation at electrostatic septum.

Fig. 17 shows particle motion during adiabatic switch on and off of the resonant sextupole. The first 1000 turns are achieved while XR is slowly fired, XR is then maintained for the next 1000 turns before being extinguished over 1000 additional turns, after what the motion ends on an ellipse that coincides with the initial linear motion.

[4]By the mean time the plot shows that, as expected in the absence of extraction septa and as long as they are within geometrical acceptance of the ring particles beyond separatrix undergo closed motion as well and stay within vacuum pipe limits.

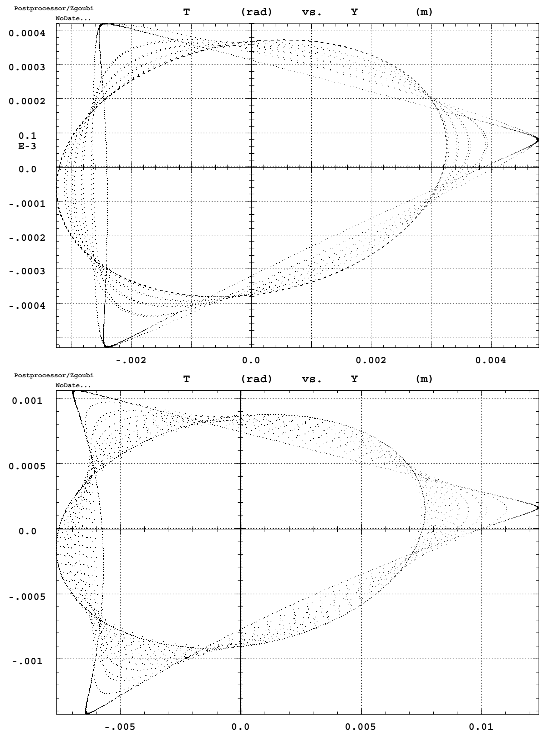

Figure 17: Adiabatic switch on (top) and off (bottom) of XR.

C Tracking inaccuracy

Two particles launched, one goes out fast, the second one shows strong emittance smear out, due to horizontal emittance increase towards instable limit arising ensuing from strongly non-symplectic tracking.

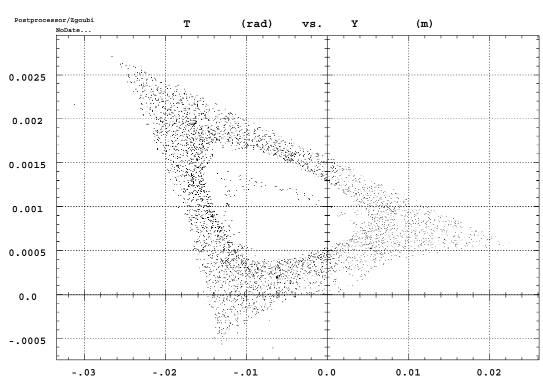

Figure 18: No acceleration here ! Non-symplectic tracking.

References

[1] Projet d'un centre d'hadronthérapie par faisceaux d'ions carbone, Mise à jour janvier 2001, M. Bajard, J. P. Gérard, J. Remillieux, D. Sappey-Marinier, UCB-Lyon 1.

[2] Proton-ion medical machine study, Part I, CERN/PS 99-010 (DI) March 1999 & Part II, CERN/PS 2000-007 (DR) May 2000.

[3] Projet de hadronthérapie à Lyon, Lignes de faisceau, B. Launé, F. Méot, A. Tkatchenko, CEA DSM DAPNIA/SEA-01-10 & CNRS IN2P3 IPNO-01-07, 4 juillet 2001.

[4] Private communication, M. Bajard, IPN, UCB-Lyon I.

[5] AGILE program for synchrotron lattice design and PIMMS data, CD release, P. J. Bryant, CERN, private communication, Nov. 2000.

[6] BETA optics code, J. Payet et als., CEA DSM/DAPNIA/SEA, Saclay.

[7] M. Pullia, Report CERN/PS 2000-006.